CHAOTIC ROTATIONS OF AN ASYMMETRIC BODY WITH TIME-DEPENDENT MOMENTS OF INERTIA AND VISCOUS DRAG

M. IÑARREA

Departamento de Física Aplicada, Universidad de La Rioja, 26004 Logroño, Spain
manuel.inarrea@dq.unirioja.es

V. LANCHARES

Departamento de Matemáticas y Computación, Universidad de La Rioja, 26004 Logroño, Spain
vlancha@dmc.unirioja.es

V. M. ROTHOS

Department of Mathematical Sciences, University of Loughborough, Loughborough LE11 3TU UK
v.m.rothos@lboro.ac.uk

J. P. SALAS

Departamento de Física Aplicada, Universidad de La Rioja, 26004 Logroño, Spain
josepablo.salas@dq.unirioja.es

We study the dynamics of a rotating asymmetric body under the influence of an aerodynamic drag. We assume that the drag torque is proportional to the angular velocity of the body. Also we suppose that one of the moments of inertia of the body is a periodic function of time and that the center of mass of the body is not modified. Under these assumptions, we show that the system exhibits a transient chaotic behavior by means of a higher dimensional generalization of the Melnikov's method. This method give us an analytical criterion for heteroclinic chaos in terms of the system parameters. These analytical results are confirmed by computer numerical simulations of the system rotations.

Keywords: Attitude dynamics; Melnikov's method.

1. Introduction

The dynamics of a rotating body is a classic topic of study in mechanics. So, in the eighteenth and nineteenth centuries, several aspects of the motion of a rotating rigid body were studied by many authors as Euler, Cauchy, Jacobi, Poinsot, Lagrange and Kovalevskaya. Many of these theoretical results have been collected in Leimanis's book [1965].

However, the study of the dynamics of rotating bodies is still very important in modern science. From a theoretical point of view, this topic offers quite interesting models and problems in the field of nonlinear dynamics. In this way, the Euler's equations of motion of a rotating body are a representative example. Moreover, the dynamics of bodies in rotation, have had many applications in the explanation of different physical phenomena as the motion of Earth's poles [Peano, 1895a, 1895b], the variation of the latitude on the surface of the Earth [Volterra, 1899], the librations of the Moon, the motion of gyrostats and gyroscopes, and the chaotic rotations of irregular shaped natural satellites as Hyperion [Wisdom *et al.*, 1984]. In the last

decades, the dynamics of rotating bodies has been the object of great interest in astrodynamics and space engineering, this is because it is an useful model to study, at first approximation, the attitude dynamics of spacecrafts [Hughes, 1986; Sidi, 1997].

Any spacecraft in orbit is under the action of several kinds of external disturbance torques as the solar radiation pressure, the gravity torque due to the Earth's gravity gradient, the magnetic torque caused by the Earth's magnetic field, or the aerodynamic torque due to the action of a resisting medium like the Earth's atmosphere [Bryson, 1994]. Although all these external disturbances are not large in comparison with the weight of the vehicle, they cannot be considered as negligible in a closer study of the attitude dynamics of a spacecraft because their influence may be significant in the real attitude motion of the vehicle. In this way, there is a range of altitudes with operative satellites at which aerodynamic drag not only is not negligible but it also may even be dominant [Hughes, 1986].

Several authors as Wainwright [1927], Deimel [1952], Gray [1959], and other ones cited in Leimanis's book [1965, pp. 206–207] have studied the dynamics of a revolving symmetric body under the influence of an aerodynamic drag. All of them assume that the action of the resisting medium surrounding the body results in a drag torque opposite to the motion and proportional to the first power of the angular velocity of the body. All these studies are also based on the premise that the rotating system is a perfectly rigid body. Unfortunately, all real materials are elastic and deformable to some degree. The model of a perfectly rigid body can lead to results not coincident with the real behavior of a spacecraft. This mistake was dramatically pointed out in 1958 when an unexpected instability appeared in the rotation of the Explorer I satellite [Wiesel, 1997, pp. 135–136].

These considerations have moved us to focus our attention on the dynamics of a rotating asymmetric body with one of its moments of inertia as a periodic function of time, and under the influence of an external aerodynamic drag torque. We also assume that the center of mass of the body is not modified. This model could be of applicability in the design of the attitude stabilization system for a spacecraft. In fact, a spacecraft with appendanges like antennas or solar panels is subjected to structural oscillations due to excitation or external torques and forces [Bryson, 1994, p. 114]. In the absence of the external drag torque, this system

has already been studied by Lanchares *et al.* [1998] and Iñarrea and Lanchares [2000]. They analyzed and described the chaotic behavior of a dual-spin spacecraft with time-dependent moments of inertia in free motion. The global dynamics of our present problem under the action of the viscous drag is actually expected. In fact the main contribution of the drag results in the despin of the body until it reaches an equilibrium position. However, the time-dependence of the moment of inertia introduces a certain chaotic dimension in the behavior of the system in such a way that the final state of the body is in some cases unpredictable.

In the study of this kind of systems the Melnikov method proves to be a powerful tool. The Melnikov method [Melnikov, 1963] is an analytical tool to determine, at first order, the existence of homo/heteroclinic intersections and so chaotic behavior in near-integrable systems. Recently, many authors have applied the Melnikov method to reveal chaotic dynamics in several problems on rotating bodies under different kinds of perturbations. In this way, Gray *et al.* [1999] have investigated a viscously damped free rigid body perturbed by small oscillating masses. Holmes and Marsden [1983], Koiller [1984], and Peng and Liu [2000] have considered free gyrostats with a slightly asymmetric rotor. Tong *et al.* [1995] have treated an asymmetric gyrostat under the uniform gravitational field. On the other hand, Salam [1987] has extended the applicability of the Melnikov method to include a general class of highly dissipative systems with a small time-sinusoidal perturbation. In order to study the persistence of the heteroclinic chaos in our rotating body in the presence of aerodynamic drag, we have made use of a higher dimensional generalization of the Melnikov method [Wiggins, 1988].

Despite analytical techniques to highlight the chaotic behavior of the system, numerical simulations are needed to confirm the predicted behavior and give a deeper understanding of the global dynamics of the system. To this end, numerical methods based on computer simulations of the body rotations by means of numerical integration of the equations of motion are performed. This allows us to establish two basically different kind of orbits which serve as a criterion to decide when the system behaves regular or chaotic. Besides, Poincaré surfaces of section are used to reveal the existence of a primary stochastic layer in the absence of aerodynamic viscous drag. Finally, a comprehensive study of the final asymptotic behavior of the system is

achieved focusing on the geometry of the attraction basins of the two asymptotic stable points. These basins are determined by propagation of thousands of orbits covering all possible initial conditions over phase space. All these numerical features show an extremely random behavior for weak aerodynamic drag.

The present paper is structured in the following way. In Sec. 2, we describe in detail the perturbed system and we also express the Euler's equations of motion of the system in the variables of the components of the angular momentum in the body frame. Then we point out the main features of the phase space of the unperturbed system in these variables, that is, the spherical phase space of the free rigid body. In Sec. 3 we describe the generalization of the Melnikov method to higher dimensional systems that we use in this study. Since in the variables of the body frame components of the angular momentum, the phase space of the perturbed system is no longer a spherical surface, in Sec. 4 we calculate the Melnikov function of the perturbed system in the Serret variables [1866]. The Melnikov function yields an analytical criterion for heteroclinic chaos in terms of the system parameters. Finally, in Sec. 5 by means of computer numerical simulations of the body motion we develop a numerical criterion to check the validity of the analytical criterion for chaos obtained through the Melnikov method. We also study in a qualitative way the chaos–order evolution of the attraction basins of the perturbed system with the strength of the aerodynamic drag.

2. Description of the System and Equations of Motion

Let us consider a rotating asymmetric body with a time-dependent moment of inertia and under the action of a small external viscous drag. We will use a body fixed orthonormal reference frame $\mathcal{B}\{O, \mathbf{b}_1, \mathbf{b}_2, \mathbf{b}_3\}$. The origin O of the body frame $\mathcal{B}$ is located at the center of mass of the body, and the directions of the orthonormal basis $(\mathbf{b}_1, \mathbf{b}_2, \mathbf{b}_3)$ coincide with the principal axes of the body.

The moments of inertia of the body are denoted by A, B, C, and we assume a triaxial body with the relation $A > B > C$. We suppose specifically that the greatest moment of inertia of the body is a periodic function of time, that is, $A = A(t)$ whereas the two other moments of inertia, B and C remain constant. Although A varies with time, we will sup-

pose that the body always holds the same triaxial condition, $A(t) > B > C$, at any time. Also we will suppose that the center of mass of the body is not altered. It is important to note that the choice of the greatest moment of inertia as function of time, and the other two constant, is not relevant in the dynamics of the problem. In fact, the results and conclusions are similar no matter which moment of inertia is supposed to be variable with time.

The function that defines the change of the body's greatest moment of inertia $A(t)$ is supposed to have the specific form

$$\frac{1}{A(t)} = a_1(t) = a_{10} + \varepsilon \cos \nu t, \qquad (1)$$

where ε is a parameter much smaller than a_{10}, ($\varepsilon \ll a_{10}$). That is, $a_1(t)$ is a periodic function with frequency ν and amplitude ε.

If we denote $\boldsymbol{\omega} = \omega_x \mathbf{b}_1 + \omega_y \mathbf{b}_2 + \omega_z \mathbf{b}_3$ as the rotation angular velocity of the body, expressed by the body frame $\mathcal{B}$, the angular momentum $\mathbf{G}$ of the body can be written as

$$\mathbf{G} = G_x \mathbf{b}_1 + G_y \mathbf{b}_2 + G_z \mathbf{b}_3 = \mathbb{I} \boldsymbol{\omega},$$

where $\mathbb{I}$ is the tensor of inertia of the body. As it is expressed in the body frame $\mathcal{B}$ of the principal axes of the body, this tensor is a diagonal one, that is, $\mathbb{I} = \mathrm{diag}(A(t), B, C)$.

We also consider that the system is in a lightly resisting medium and its action on the rotating body is a small drag torque $\mathbf{N}$ opposite to the motion. For the sake of simplicity we assume that the torque is directly proportional to the angular velocity of the body, that is,

$$\mathbf{N} = -\gamma \boldsymbol{\omega} = -\gamma \mathbb{I}^{-1} \mathbf{G},$$

where $\gamma > 0$ is the coefficient of the viscous drag.

Under all these assumptions, and by means of the classical angular momentum theorem, the Eulerian equations of motion of the system expressed in terms of the angular momentum components (G_x, G_y, G_z) can be easily obtained

$$\begin{aligned}
\dot{G}_x &= (a_3 - a_2)G_y G_z - \gamma a_1(t)G_x \\
&= (a_3 - a_2)G_y G_z - \gamma a_{10}G_x - \gamma \varepsilon G_x \cos \nu t, \\
\dot{G}_y &= (a_1(t) - a_3)G_x G_z - \gamma a_2 G_y \\
&= (a_{10} - a_3)G_x G_z + \varepsilon G_x G_z \cos \nu t - \gamma a_2 G_y, \\
\dot{G}_z &= (a_2 - a_1(t))G_x G_y - \gamma a_3 G_z \\
&= (a_2 - a_{10})G_x G_y - \varepsilon G_x G_y \cos \nu t - \gamma a_3 G_z.
\end{aligned} \qquad (2)$$

where $a_2 = 1/B$ and $a_3 = 1/C$.

As we assume a small variation of the greatest moment of inertia $A(t)$, that is, ($\varepsilon \ll a_{10}$), and also a small drag torque ($\gamma \ll 1$), we can consider these features of the system as small perturbations. In this way, the unperturbed system coincides with the triaxial rigid body in free motion. The Euler's equations of motion of the free rigid body are given by

$$\dot{G}_x = (a_3 - a_2)G_y G_z \,,$$
$$\dot{G}_y = (a_{10} - a_3)G_x G_z \,, \qquad (3)$$
$$\dot{G}_z = (a_2 - a_{10})G_x G_y$$

and they are just Eqs. (2) when $\varepsilon = \gamma = 0$. As it is well known, the free rigid body problem has three degrees of freedom and the system admits two integrals: the energy and the angular momentum, therefore it is an integrable problem.

Indeed, in the free rigid body problem, by virtue of the angular momentum theorem, the angular momentum $\mathbf{G}$ is constant in an inertial frame $\mathcal{S}$ fixed in the space, and consequently its norm G is also constant. As it is well known, the change from the space frame $\mathcal{S}$ to the body frame $\mathcal{B}$ may be directly done by means of one rotation about the origin O. Thus, as the norm of a vector is invariant under the action of the group SO(3) of rotations, the norm G is also constant in the body frame $\mathcal{B}$, that is, $G = \sqrt{G_x^2 + G_y^2 + G_z^2} = $ cte. It can be easily checked making use of Eqs. (3), since

$$\dot{G} = \frac{1}{G}(G_x \dot{G}_x + G_y \dot{G}_y + G_z \dot{G}_z) = 0 \,.$$

Therefore, in the variables (G_x, G_y, G_z), the phase space of the system may be regarded as a foliation of invariant manifolds

$$S^2(G) = \{(G_x, G_y, G_z) | G_x^2 + G_y^2 + G_z^2 = G^2\} \,.$$

The total angular momentum $\mathbf{G}$ in the body frame $\mathcal{B}$ describes a curve on the S^2 sphere of radius G. From Eqs. (3), it is also easy to deduce that there are six equilibria located at the intersections of the body frame axes with the sphere S^2. The two equilibria located at the axis $\mathbf{b}_2$, of intermediate moment of inertia are unstable equilibria, whereas the other four equilibria are stable. The two unstable equilibria, denoted by E_1 and E_2, are connected by four heteroclinic trajectories. These orbits are the separatrices of the phase space. Figure 1 shows the main features of the phase flow for the triaxial rigid body in free rotation in the spherical phase space S^2.

These separatrices divide the phase space into two different classes of motion: circulations about the axis $\mathbf{b}_1$ of maximal moment of inertia; and circulations about the axis $\mathbf{b}_3$ of minimal moment of inertia. The explicit expressions of the different types of trajectories can be obtained in terms of elliptic and hyperbolic functions, from Eqs. (3) by means of the two integrals of the unperturbed problem: the energy and the angular momentum (for more details see [Deprit & Elipe, 1993]). The solutions corresponding to the four asymptotic heteroclinic trajectories, are

$$\begin{cases} G_x^* = (-1)^{[(k-1)/2]}G^*\sqrt{\dfrac{a_3 - a_2}{a_3 - a_{10}}}\,\text{sech}(n_2 t)\,, \\[2mm] G_y^* = (-1)^{k-1}G^*\tanh(n_2 t)\,, \qquad\qquad k = 1, 2, 3, 4\,. \\[2mm] G_z^* = (-1)^{[k/2]}G^*\sqrt{\dfrac{a_2 - a_{10}}{a_3 - a_{10}}}\,\text{sech}(n_2 t) \end{cases} \qquad (4)$$

where

$$n_2 = \sqrt{(a_2 - a_{10})(a_3 - a_2)} \qquad (5)$$

and $[b]$ stands for the integer part of b.

3. Higher Dimensional Melnikov Method

The idea of a first-order perturbation calculation for the detection of transverse intersections of stable and unstable manifolds of invariant sets in near-integrable Hamiltonian systems may be proved, at first order, by means of the Melnikov's method [Melnikov, 1963]. For detailed descriptions of geometric approach to
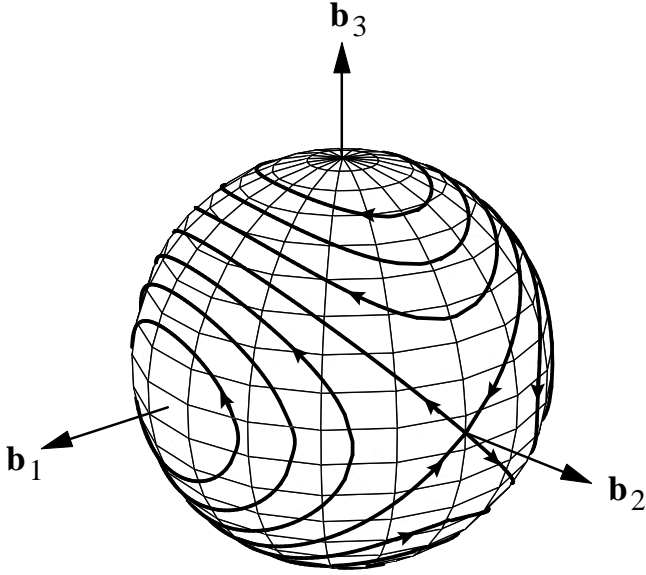
Fig. 1. The phase flow for the triaxial rigid body in free rotation ($a_{10} < a_2 < a_3$) in the (G_x, G_y, G_z) variables.

perturbations of planar homoclinic orbits based on this method see [Guckenheimer & Holmes, 1983]. Higher dimensional generalizations of the Melnikov method appear in [Wiggins, 1988].

Consider the system of differential equations

$$\dot{x} = JD_x\mathcal{H}(x, I) + \varepsilon g^x(x, I, \theta; \mu),$$
$$\dot{I} = \varepsilon g^I(x, I, \theta; \mu), \qquad (6)$$
$$\dot{\theta} = \Omega(x, I) + \varepsilon g^\theta(x, I, \theta; \mu)$$

with $(x, I, \theta) \in \mathbb{R}^{2n} \times \mathbb{R}^m \times T^l$, $\mu \in \mathbb{R}^\rho$ is a vector of parameters, $0 \leq \varepsilon \ll 1$, and (g^x, g^I, g^θ) is 2π-periodic in θ.

The system obtained by setting $\varepsilon = 0$ in (6) is referred to as the unperturbed system which we write below:

$$\dot{x} = JD_x\mathcal{H}(x, I), \quad \dot{I} = 0, \quad \dot{\theta} = \Omega(x, I) \qquad (7)$$

with Hamiltonian function $\mathcal{H}$. The system (7) is a completely integrable Hamiltonian system with n scalar valued integrals $\mathcal{H} = K_1, \ldots, K_n$. Note the structure of (7): the x-component of (7) decouples from the I and θ components of (7). The dynamics of the I and θ components of (7) are quite simple and we make the following assumptions on the dynamics of the x-components of (7):

For all $I \in U \subset \mathbb{R}^m$ (U be an open subset), the equations:

$$\dot{x} = JD_x\mathcal{H}(x, I) \qquad (8)$$

has a hyperbolic fixed point $\tilde{x}_0(I)$, connected to itself by a homoclinic orbit $x_h(t, I)$:

$$\lim_{t \to \pm\infty} x_h(t, I) = \tilde{x}_0(I).$$

We can draw the following conclusions concerning the phase space structure of (7) in the full $(2n + m + l)$ dimensional phase space.

The set of points $\mathcal{M}$ in $\mathbb{R}^{2n} \times \mathbb{R}^m \times T^l$ defined by

$$\mathcal{M} = \{(x, I, \theta) \in \mathbb{R}^{2n} \times \mathbb{R}^m \times T^l : x = \tilde{x}(I),\} \qquad (9)$$

is a C^r $(m + l)$-dimensional normally hyperbolic invariant manifold of the unperturbed system which has the structure of m parameter family of l-dimensional tori $\tau(\bar{I})$. We denote $\tau_\varepsilon(\bar{I})$ the l-dimensional normally hyperbolic invariant torus contained in $\mathcal{M}_\varepsilon$ having a stable $W^s(\tau(\bar{I}))$ and unstable $W^u(\tau(\bar{I}))$ manifolds. Moreover, $W^s(\tau(\bar{I})) \subset W^s(\mathcal{M})$ and $W^u(\tau(\bar{I})) \subset W^u(\mathcal{M})$. The term normally hyperbolic invariant manifold means that the rate of expansion and contraction under the linearized analysis in directions complementary to $\mathcal{M}$ dominates those in directions tangent to $\mathcal{M}$. The important point for us is that normally hyperbolic invariant sets persist under perturbations and denote $\mathcal{M}_\varepsilon$ as the perturbed manifold. Moreover, $\mathcal{M}$ has C^r $(n + m + l)$-dimensional manifolds $W^s(\mathcal{M})$, $W^u(\mathcal{M})$, which intersect along the $(n + m + l)$-dimensional homoclinic (or heteroclinic) manifold

$$\Gamma = \{(x_h(-t_0, a), I, \theta_0) \in \mathbb{R}^{2n} \times \mathbb{R}^m$$
$$\times T^l / (t_0, a, I, \theta_0) \in \mathbb{R} \times \mathbb{R}^{n-1} \times U \times T^l\}$$

where (t_0, a) is a parametrization of the homoclinic manifold and $W^{s,u}(\tau(\bar{I})) \subset W^{s,u}(\mathcal{M})$, Fig. 2. We define a moving coordinate system along the homoclinic manifold Γ of the unperturbed system which will be useful to determine the splitting of the manifolds in the perturbed system.

For a given $(t_0, a, I, \theta_0) \in \mathbb{R} \times \mathbb{R} \times \mathbb{R}^m \times T^l$, let $p = (x^I(t_0, a), I, \theta)$ denote the corresponding point on $\Gamma = W^s(\mathcal{M}) \cap W^u(\mathcal{M}) \setminus \mathcal{M}$. For any point $p \in \Gamma$, let Π_p denote the $(n + m)$-dimensional plane spanned by the vectors $\{((D_x K_i, 0), \hat{I}_i), i = 1, \ldots, n\}$ and $\hat{I}_i$ represent unit vectors in the I_i directions and $D_x K_i$ are evaluated at p. Thus, varying p serves to move the plane Π_p along the homoclinic orbit Γ, Fig. 3.

From the geometry of our problem we obtain that $W^s(\mathcal{M})$ intersects Π_p transversely in a m-dimensional surface which is referred to as S_p^s
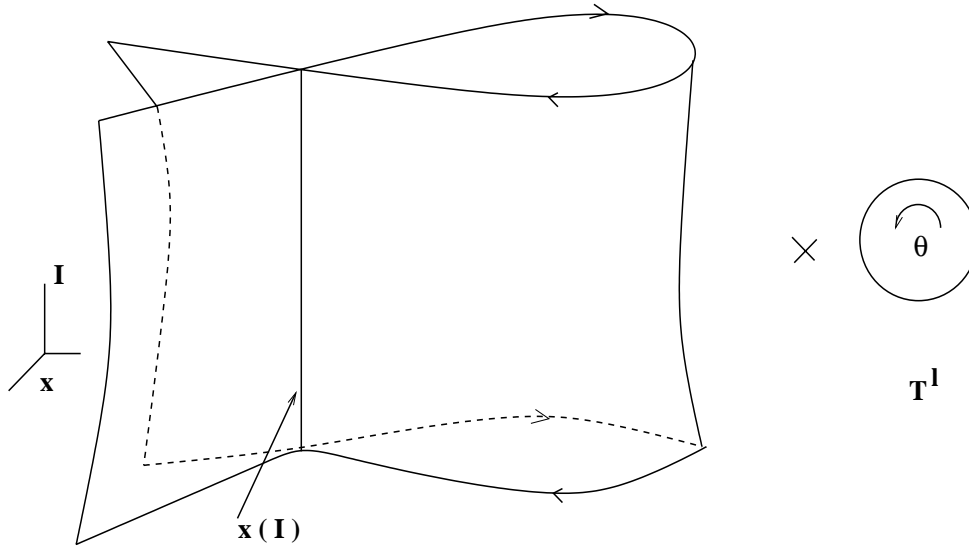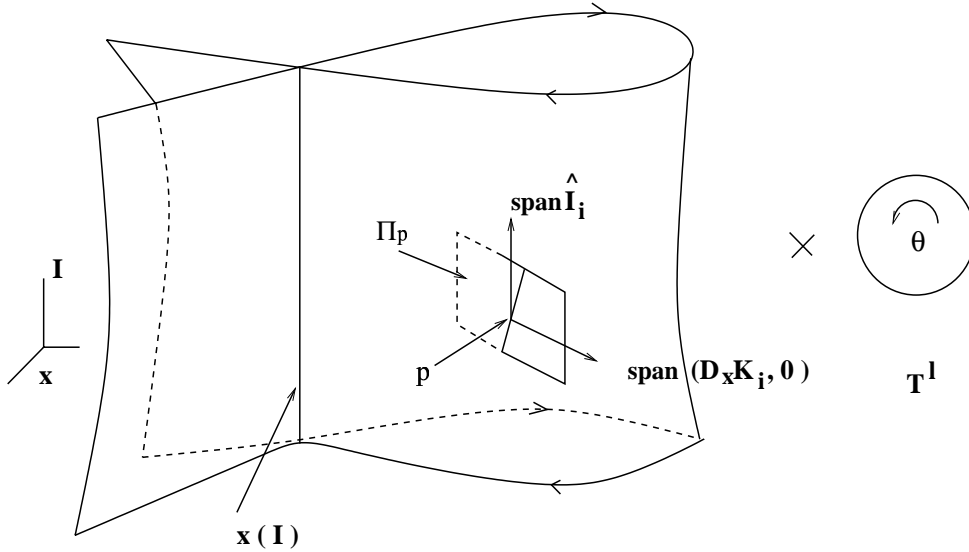
Fig. 2.   The unperturbed phase space of (7).

Fig. 3.   Geometry of Π_p.

(similar S_p^u). Moreover since $W^s(\mathcal{M})$ and $W^u(\mathcal{M})$ coincide along Γ, we have $S_p^s = S_p^u$, for every $p \in \Gamma$.

For ε sufficiently small, $W^s(\mathcal{M}_\varepsilon)$ (resp. $W^s(\mathcal{M}_\varepsilon)$) intersect Π_p in a m-dimensional surface $S_p^{s,\varepsilon}$(resp. $S_p^{u,\varepsilon}$). The measurement of distance between the stable and unstable manifolds of the invariant torus is constructed by choosing points $p_\varepsilon^s \in S_p^{s,\varepsilon}$ and $p_\varepsilon^u \in S_p^{u,\varepsilon}$ where $p_\varepsilon^{u,s} = (x_\varepsilon^{u,s}, I_\varepsilon^{u,s})$ with $I_\varepsilon^u = I_\varepsilon^s$, at the point p are defined by

$$d^{\bar{I}} = |p_\varepsilon^u - p_\varepsilon^s| = |x_\varepsilon^u - x_\varepsilon^s|$$

Following Wiggins [1988], the components of distance vector along the directions $(D_x K_i, 0)$ is defined as follows:

$$d_i^{\bar{I}} = \frac{\langle D_x K_i(x_h(t_0, a), \bar{I}), x_\varepsilon^u - x_\varepsilon^s \rangle}{\|D_x K_i(x_h(t_0, a), \bar{I})\|}, \quad i = 1, \ldots, n.$$

The Melnikov vector for the system (6) is given by

$$\mathbf{M}(\theta_0, \bar{I}, a, \mu)$$
$$= (M_1(\theta_0, \bar{I}, a, \mu), \ldots, M_n(\theta_0, \bar{I}, a, \mu)) \quad (10)$$

where

$$M_i(\theta_0, \overline{I}, a, \mu) = \int_{-\infty}^{\infty} [\langle D_x K_i, g^x \rangle$$

$$+ \langle D_I K_i, g^I \rangle](q_0(\overline{I}, t), \mu; 0)dt$$

$$- \langle D_I K_i(\gamma(\overline{I}), \overline{I}),$$

$$\int_{-\infty}^{\infty} g^I(q_0(\overline{I}, t), \mu; 0)dt\rangle \quad (11)$$

$q_0(t) = (x^{\overline{I}}(t, a), \overline{I}, \int^t \Omega(x^{\overline{I}}(s, a))ds + \theta_0)$ is the solution on the unperturbed separatrix and $\langle , \rangle$ denotes the inner product in $\mathbb{R}^n$.

Theorem 1. [Wiggins, 1988] *Suppose there exists a point:*

$$(\theta_0, \alpha, \mu) = (\overline{\theta}_0, \overline{a}, \overline{\mu}) \in T^l \times \mathbb{R}^{n-1} \times \mathbb{R}^p$$

with

$$l + n - 1 + p \geq n$$

such that

- $\mathbf{M}(\overline{\theta}_0, \overline{I}, \overline{\alpha}, \overline{\mu}) = 0$
- *rank* $D\mathbf{M}(\overline{\theta}_0, \overline{I}, \overline{\alpha}, \overline{\mu}) = n$
- *rank* $D_{(\theta_0, \alpha)}\mathbf{M}(\overline{\theta}_0, \overline{I}, \overline{\alpha}, \overline{\mu}) = n$

Then, for ε sufficiently small, the invariants manifolds $W^s(\tau_\varepsilon(\overline{I})) \subset W^s(\mathcal{M}_\varepsilon)$ and $W^u(\tau_\varepsilon(\overline{I})) \subset W^u(\mathcal{M}_\varepsilon)$ intersect transversely near $(\overline{\theta}_0, \overline{a})$.

Analogous techniques for detecting heteroclinic orbits, in the same class of systems, can be developed precisely in the same manner. The only difference is that the unperturbed system is assumed to have *two normally hyperbolic invariant manifolds*, say $\mathcal{M}_1$ and $\mathcal{M}_2$, which are connected to each other by a manifold of heteroclinic orbits. The geometry of the splitting of the manifolds and the Melnikov vector are the same as in the homoclinic case for orbits heteroclinic to tori of the *same dimension*.

4. Chaotic Motion. The Melnikov Function

The extended Melnikov method introduced in the previous section is the basic tool we need to analyze the possible chaotic dynamics of the system (2). As mentioned in Sec. 2, the unperturbed problem is that of a rigid body in free motion and the stable and unstable manifolds, corresponding to the two
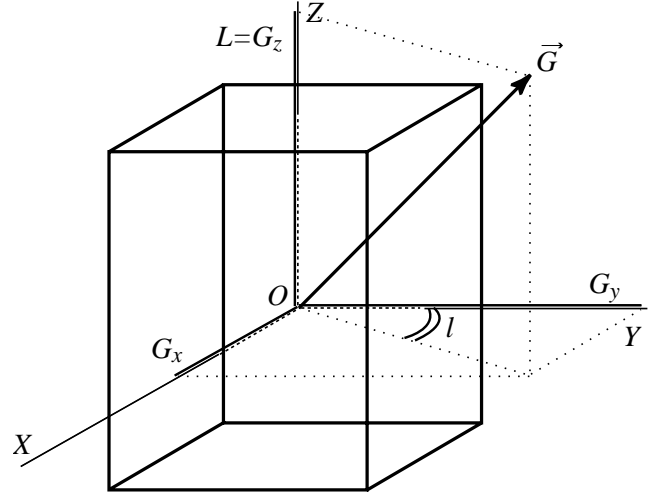

Fig. 4. Relation between the cartesian components of the vector **G** and the Serret variables.

unstable equilibria, join smoothly. However, under a small perturbation, these two manifolds are not forced to coincide and it is possible that they intersect transversely and a heteroclinic tangle is generated giving rise to chaotic behavior.

Consider now the perturbed system, that is, the rotating body with its greatest moment of inertia $A(t)$ as a periodic function of time ($\varepsilon \neq 0$), and under the action of a small drag torque ($\gamma \neq 0$). Since in this case there exists an external torque, now the norm G of the angular momentum of the body is not constant. Therefore, in the (G_x, G_y, G_z) variables the phase space of the perturbed system is no longer a spherical surface S^2. This fact has moved us to make use of another set of coordinates, the so-called Serret variables [1866] (l, L, G). These coordinates, that have been used in the study of the free rigid body [Deprit & Elipe, 1993], are like cylindrical coordinates of vector **G** (see Fig. 4) and so they are related to (G_x, G_y, G_z) through the following equations

$$G_x = \sqrt{G^2 - L^2} \sin l,$$
$$G_y = \sqrt{G^2 - L^2} \cos l, \quad (12)$$
$$G_z = L.$$

In the Serret variables, the phase space of the triaxial free rigid body is the plane (l, L) shown in Fig. 5.

Taking into account the coordinate transformation Eqs. (12), it is possible to write the equations of motion of the unperturbed free rigid problem (3)
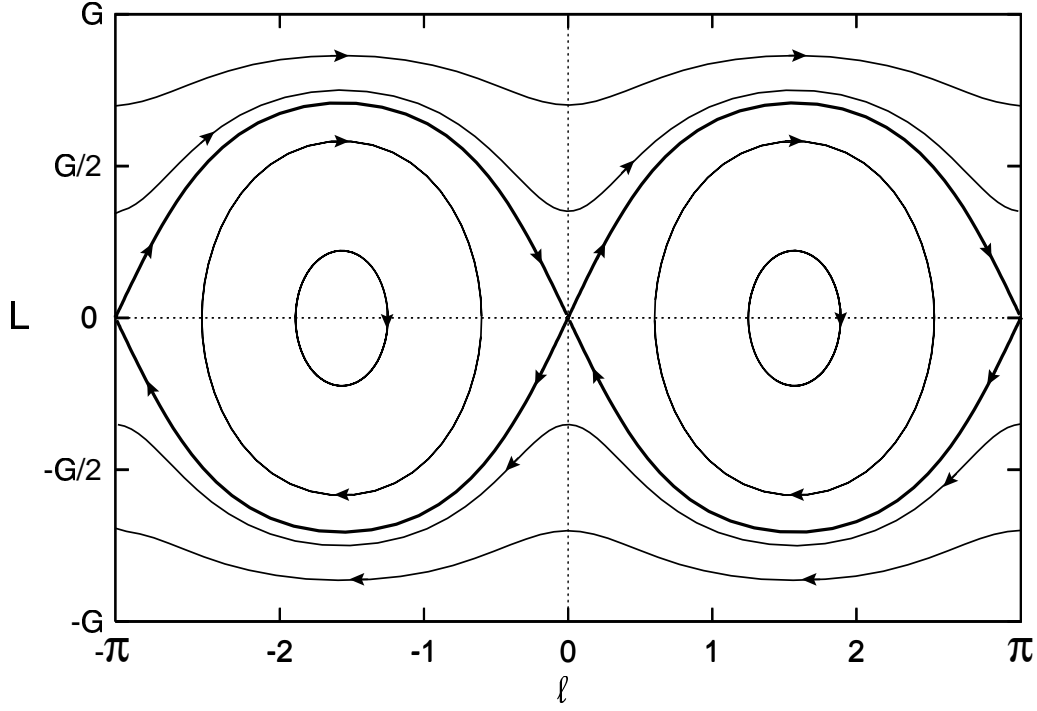
Fig. 5.   The phase plane of the triaxial rigid body in free rotation ($a_{10} < a_2 < a_3$) in the (l, L) Serret variables.

in terms of the Serret variables as

$$\dot{l} = (a_3 - a_{10} \sin^2 l - a_2 \cos^2 l)L\,,$$
$$\dot{L} = (a_2 - a_{10})(G^2 - L^2) \sin l \cos l\,, \qquad (13)$$
$$\dot{G} = 0\,.$$

As we said above, the unperturbed system (13) is integrable, and its Hamiltonian written in the Serret variables results in

$$\mathcal{H}(l, L, G) = \frac{1}{2}[a_3 L^2 + a_2(G^2 - L^2) \cos^2 l$$
$$- a_{10}(G^2 - L^2) \sin^2 l]\,. \qquad (14)$$

In the same way, making use of Eqs. (12) and neglecting terms of $\mathcal{O}(\varepsilon\gamma)$ order, the equations of motion of the perturbed system expressed in the (l, L, G) coordinates are given by

$$\dot{l} = (a_3 - a_{10} \sin^2 l - a_2 \cos^2 l)L - \varepsilon L \sin^2 l \cos \nu t$$
$$+ \gamma(a_2 - a_{10}) \sin l \cos l + \mathcal{O}(\varepsilon\gamma)\,,$$
$$\dot{L} = (a_2 - a_{10})(G^2 - L^2) \sin l \cos l$$
$$- \varepsilon(G^2 - L^2) \sin l \cos l \cos \nu t - \gamma a_3 L\,,$$
$$\dot{G} = -\frac{\gamma}{G}[a_3 L^2 + a_2(G^2 - L^2)$$
$$+ (a_{10} - a_2)(G^2 - L^2) \sin^2 l] + \mathcal{O}(\varepsilon\gamma)\,. \qquad (15)$$

In order to apply the generalization of Melnikov's method, Eqs. (15) may be written in a more convenient form, (cf. (6)). If we define the new parameter $\hat{\gamma} = \gamma/\varepsilon$, it is possible to consider ε as the only small parameter of our system. In this way, the equations of motion of the perturbed system can be expressed as

$$\dot{l} = (a_3 - a_{10} \sin^2 l - a_2 \cos^2 l)L$$
$$+ \varepsilon[-L \sin^2 l \cos \theta + \hat{\gamma}(a_2 - a_{10}) \sin l \cos l]\,,$$
$$\dot{L} = (a_2 - a_{10})(G^2 - L^2) \sin l \cos l$$
$$+ \varepsilon[-(G^2 - L^2) \sin l \cos l \cos \theta - \hat{\gamma}a_3 L]\,,$$
$$\dot{G} = -\varepsilon\frac{\hat{\gamma}}{G}[a_3 L^2 + a_2(G^2 - L^2)$$
$$+ (a_{10} - a_2)(G^2 - L^2) \sin^2 l]\,,$$
$$\dot{\theta} = \nu\,. \qquad (16)$$

These equations can be set up in a more compact form as follows

$$\dot{\mathbf{x}} = \mathbf{J}D_x\mathcal{H}(x, G) + \varepsilon\mathbf{g}^x(\mathbf{x}, G, \nu, \hat{\gamma})\,,$$
$$\dot{G} = \varepsilon g^G(\mathbf{x}, G, \hat{\gamma})\,, \qquad (17)$$
$$\dot{\theta} = \nu$$

where we make use of the following notation

$$\mathbf{z} = (\mathbf{x} := (l, L), G, \theta) \in S^1 \times \mathbb{R} \times \mathbb{R} \times S^1 \quad \mathbf{J} = \begin{pmatrix} 0 & 1 \\ -1 & 0 \end{pmatrix} \quad D_x \mathcal{H} = \left(\frac{\partial \mathcal{H}}{\partial l}, \frac{\partial \mathcal{H}}{\partial L} \right)$$

$$\frac{\partial \mathcal{H}}{\partial l} = (a_{10} - a_2)(G^2 - L^2) \sin l \cos l$$

$$\frac{\partial \mathcal{H}}{\partial L} = L(a_3 - a_2 \cos^2 l - a_{10} \sin^2 l) = (a_3 - a_2)L + (a_2 - a_{10})L \sin^2 l \tag{18}$$

$$\mathbf{g}^x = \begin{pmatrix} g^l \\ g^L \end{pmatrix} = \begin{pmatrix} -L \sin^2 l \cos \theta + \hat{\gamma}(a_2 - a_{10}) \sin l \cos l \\ -(G^2 - L^2) \sin l \cos l \cos \theta - \hat{\gamma} a_3 L \end{pmatrix}$$

$$g^G = -\frac{\hat{\gamma}}{G}[a_3 L^2 + a_2(G^2 - L^2) + (a_{10} - a_2)(G^2 - L^2) \sin^2 l]$$

In order to apply Theorem 1, we need to define the associate Poincaré map for each fixed $l_0 > 0$ and given constants of motion $\mathcal{H}$, G. First of all, we construct at the point $\mathbf{z}_0 = \mathbf{z}^*(l_0, L, G, \theta)$, on the unperturbed heteroclinic manifold, an orthonormal frame of reference given by the four unit vectors

$$\mathbf{n}_\mathcal{H} = \frac{D_x \mathcal{H}}{\|D_x \mathcal{H}\|}, \quad \mathbf{n}_G,$$

$$\mathbf{m}_\mathcal{H} = \mathbf{J} \eta_\mathcal{H}, \quad \mathbf{m}_G = \mathbf{J} \mathbf{n}_G$$

so that $\mathbf{n}_G$ is orthogonal to $\mathbf{n}_\mathcal{H}$, $\| \ \|$ denotes the standard Euclidean norm, and $\mathbf{J}$ the simplectic matrix given above. The unit vector $\mathbf{n}_\mathcal{H}$ is normal to $W^s(\mathcal{M}_0) \cap W^u(\mathcal{M}_0)$ at any given point (except for points on $\mathcal{M}_0$), and the remaining three unit vectors span the tangent space of $W^s(\mathcal{M}_0) \cap W^u(\mathcal{M}_0)$ at any given point. In this way, the surface of the section (Π_l) is a three-dimensional hyperplane spanned by the three vectors $\mathbf{n}_\mathcal{H}$, $\mathbf{n}_G$, $\mathbf{m}_G$ (see Fig. 3), that is,

$$\Pi_{z_0} := \{\mathbf{z} \,|\, \mathbf{z} = \mathbf{z}_0 + a_\mathcal{H} \mathbf{n}_\mathcal{H} + a_G \mathbf{n}_G$$
$$+ b_G \mathbf{m}_G, \forall a_\mathcal{H}, a_G, b_G \in \mathbb{R}\}. \tag{19}$$

Several points about Π_{z_0} should be emphasized:

(a) the vector $\mathbf{z} = \mathbf{z}_0 + b_\mathcal{H} \mathbf{J} D_x \mathcal{H}$, $b_\mathcal{H} \in \mathbb{R}$, is normal to the hyperplane Π_{z_0},
(b) for ε sufficiently small, the unperturbed vector field $\mathbf{J} D_x \mathcal{H}$ is transverse to the hyperplane Π_{z_0} and
(c) by the persistence of transversal intersections, it follows that the perturbed vector field $\mathbf{J} D_x \mathcal{H} + \varepsilon \mathbf{g}$ is transverse to the hyperplane Π_{z_0}, Fig. 6.

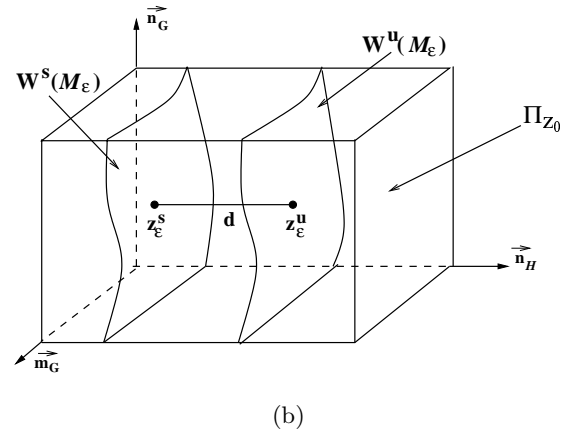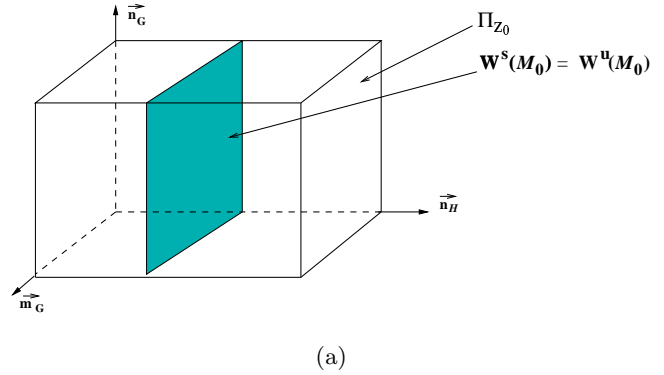It is on this surface of section where the distance between stable and unstable manifolds along

(a)

(b)

Fig. 6. (a) The intersection of the unperturbed manifolds with Π_{z_0}. (b) The intersection of the perturbed manifolds with Π_{z_0} and the points z_ε^u and z_ε^s.

the direction $(D_x \mathcal{H}, 0)$ is measured. At established in Sec. 2, this distance is given by

$$d_k = \frac{\langle D_x \mathcal{H}(\mathbf{x}^*(t), G^*), z_\varepsilon^u - z_\varepsilon^s \rangle}{\|D_x \mathcal{H}(\mathbf{x}^*(t), G^*)\|} \tag{20}$$

where $\mathbf{x}^*(t)$, G^* are the solutions, in the Serret variables, corresponding to the asymptotic heteroclinic

trajectories of the unperturbed system. Moreover, the distance function (20) can be expressed through the Melnikov function $M(t_0)$ as

$$d_k = \frac{\varepsilon M(t_0, b)}{\|D_x \mathcal{H}(\mathbf{x}^*(t), G^*)\|}, \quad b = (\nu, \hat{\gamma}, a_{10}, a_2, a_3),$$

where the Melnikov function $M(t_0, b)$ is

$$M(t_0, b) = \int_{-\infty}^{\infty} [\langle D_x \mathcal{H}, \mathbf{g}^x \rangle$$
$$+ \langle D_G \mathcal{H}, g^G \rangle](\mathbf{x}^*(t), G^*, t + t_0) dt$$
$$- \langle D_G \mathcal{H}(\Gamma(G^*), G^*),$$
$$\int_{-\infty}^{\infty} g^G(\mathbf{x}^*(t), G^*, t + t_0) dt \rangle$$

where $\Gamma(G^*)$ solves the set of equations $D_x \mathcal{H} = 0$ and subjected to the condition $\det[D_x^2 \mathcal{H}(\Gamma(G), G)] \neq 0$, $D_x^2 \mathcal{H}$ being the Jacobian matrix of the unperturbed system. These fixed points $\Gamma(G^*) = (\bar{l}, \bar{L})$ are $(0, 0)$ and $(\pm \pi, 0)$. Therefore,

$$D_G \mathcal{H}(\Gamma(G^*), G^*) = G^*(a_2 \cos^2 \bar{l}$$
$$- a_{10} \sin^2 \bar{l}) = G^* a_2. \quad (21)$$

In this way, the Melnikov function $M(t_0)$ give us a measure of the distance between the stable and unstable manifolds of the perturbed hyperbolic fixed point/s. Therefore as we said above, evaluating $M(t_0)$, it is possible to determine, at first order, if there are homoclinic/heteroclinic intersections and so chaotic behavior in the perturbed system. The condition for transverse intersections between the stable and unstable trajectories, and therefore for homoclinic/heteroclinic chaos is that the Melnikov function changes sign at some t_0.

For convenience in computation we can express the Melnikov function $M(t_0)$ as a sum of two terms $M(t_0) = M_1 + M_2$ where

$$M_1 = \int_{-\infty}^{\infty} \langle D_x \mathcal{H}, \mathbf{g}^x \rangle (\mathbf{x}^*(t), G^*, t + t_0) dt \quad (22)$$

and

$$M_2 = \int_{-\infty}^{\infty} \langle D_G \mathcal{H}, g^G \rangle (\mathbf{x}^*(t), G^*, t + t_0) dt$$
$$- \langle D_G \mathcal{H}(\Gamma(G^*), G^*),$$
$$\int_{-\infty}^{\infty} g^G(\mathbf{x}^*(t), G^*, t + t_0) dt \rangle. \quad (23)$$

We begin computing the first term $M_1(t_0)$. Taking into account Eqs. (14) and (18) $M_1(t_0)$ results in

$$M_1(t_0) = M_{11} + M_{12} = (a_2 - a_3) \int_{-\infty}^{\infty} (G^{*2}$$
$$- L^{*2}) L^* \sin l^* \cos l^* \cos[\nu(t + t_0)] dt$$
$$- \hat{\gamma} \int_{-\infty}^{\infty} [a_3(a_3 - a_2) L^{*2}$$
$$+ a_3(a_2 - a_{10}) L^{*2} \sin^2 l^*$$
$$+ (a_2 - a_{10})^2 (G^{*2}$$
$$- L^{*2}) \sin^2 l^* \cos^2 l^*] dt. \quad (24)$$

The very first integral M_{11} would be the Melnikov function corresponding to the system in the absence of external viscous drag. This particular case, $(\gamma = 0)$, has already been studied by Lanchares *et al.* [1998] and Iñarrea and Lanchares [2000]. They analyzed and described the chaotic behavior of a dual-spin spacecraft with time-dependent moments of inertia in free motion. That problem, when the rotor of the spacecraft is at relative rest, coincides with our present system for $(\gamma = 0)$. In those references, the authors calculated the Melnikov function $M_{11}(t_0)$ using the (G_x, G_y, G_z) variables and the solutions (4) corresponding to the unperturbed heteroclinic trajectories. In that way, making use of Eqs. (12) integral M_{11} may be written as

$$M_{11}(t_0) = \int_{-\infty}^{\infty} (a_2 - a_3) G_x^* G_y^* G_z^* \cos[\nu(t + t_0)] dt$$
$$= \frac{G^{*3}(a_3 - a_2) \pi \nu^2}{2(a_3 - a_{10}) n_2^2 \sinh\left(\dfrac{\pi \nu}{2n_2}\right)} \sin \nu t_0. \quad (25)$$

From this last Eq. (25) it is easy to see that the Melnikov function, $M_{11}(t_0)$, has simple zeroes for $\nu t_0 = k\pi$ with $k = 0, 1, 2, \ldots$. Therefore, when $\gamma = 0$ and $\varepsilon \neq 0$, the perturbation produces heteroclinic intersections between the stable and unstable manifolds of the hyperbolic equilibria E_1 and E_2. So, the perturbation generates a layer of chaotic motion surrounding the unperturbed separatrices. This stochastic layer may be observed by means of a Poincaré surface of section. The surface consists of time sections $t = \text{cte.}(\text{mod } T)$ of the third-dimensional (l, L, t) extended phase space. Figure 7 shows the presence of a stochastic layer around the unperturbed separatrices. As it can be seen in this figure, the regular trajectories appear as closed curves, whereas chaotic ones appears like a cloud of
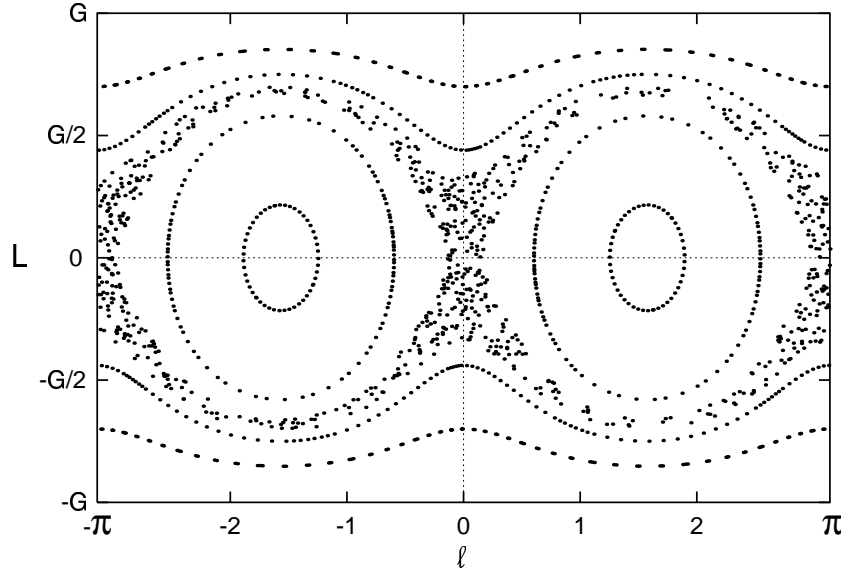
Fig. 7. Poincaré surface of section for $a_{10} = 0.1$, $a_2 = 0.2$, $a_3 = 0.3$, $\varepsilon = 0.01$, $\gamma = 0$ and $\nu = 0.1$.

points around the separatrices of the unperturbed problem.

Let us consider now the second integral M_{12} of Eq. (25). We know through Eqs. (4) the solutions of the unperturbed heteroclinic trajectories in terms of the (G_x, G_y, G_z) variables. Therefore, in order to evaluate the integral M_{12} in an easier way, it is better to express it in those variables. So, making use of Eqs. (12), M_{12} is given as

$$M_{12} = -\hat{\gamma} \int_{-\infty}^{\infty} \left[a_3(a_3 - a_2)G_z^{*2} + a_3(a_2 - a_{10})\frac{G_x^{*2}G_z^{*2}}{G_x^{*2} + G_y^{*2}} + (a_2 - a_{10})^2 \frac{G_x^{*2}G_y^{*2}}{G_x^{*2} + G_y^{*2}} \right] dt \,,$$

$$M_{12} = -\hat{\gamma}[a_3(a_3 - a_2)I_1 + a_3(a_2 - a_{10})I_2 + (a_2 - a_{10})^2 I_3] \,. \tag{26}$$

Taking into account Eqs. (4), these integrals I_i may be written as

$$I_1 = \int_{-\infty}^{\infty} G_z^{*2} dt = G^{*2} \left(\frac{a_2 - a_{10}}{a_3 - a_{10}} \right) \int_{-\infty}^{\infty} \operatorname{sech}^2(n_2 t) dt \,,$$

$$I_2 = \int_{-\infty}^{\infty} \frac{G_x^{*2}G_z^{*2}}{G_x^{*2} + G_y^{*2}} \, dt = G^{*2} \frac{n_2^2}{(a_3 - a_{10})^2} \int_{-\infty}^{\infty} \frac{dt}{\cosh^2(n_2 t)[D + \sinh^2(n_2 t)]} \,, \tag{27}$$

$$I_3 = \int_{-\infty}^{\infty} \frac{G_x^{*2}G_y^{*2}}{G_x^{*2} + G_y^{*2}} \, dt = G^{*2} D \int_{-\infty}^{\infty} \frac{\sinh^2(n_2 t)}{\cosh^2(n_2 t)[D + \sinh^2(n_2 t)]} dt \,,$$

where $D = a_3 - a_2/a_3 - a_{10}$.

These four integrals have been calculated using hyperbolic identities via reduction to easier integrals of simple fractions of hyperbolic functions, that are tabulated, e.g. [Gradshteyn & Ryzhik, 1980]. In this way, we obtain

$$I_1 = G^{*2} \frac{2(a_2 - a_{10})}{n_2(a_3 - a_{10})} \,,$$

$$I_2 = G^{*2} \frac{2(a_3 - a_2)}{n_2(a_{10} - a_3)} \left[1 - \frac{a_3 - a_{10}}{n_2} \arctan(Z) \right] \,, \tag{28}$$

$$I_3 = G^{*2} \frac{2(a_3 - a_2)}{n_2(a_{10} - a_2)} \left[\frac{a_3 - a_2}{n_2} \arctan(Z) - 1 \right] \,,$$

where

$$Z = \sqrt{\frac{a_2 - a_{10}}{a_3 - a_2}}.$$

Therefore, substituting these results into Eq. (26), the integral M_{12} yields

$$M_{12} = -2\hat{\gamma} G^{*2}[n_2 + a_2 \arctan(Z)].$$

Thus the term $M_1(t_0)$ of the complete Melnikov function results in

$$M_1(t_0) = M_{11} + M_{12}$$
$$= \frac{G^{*3}(a_3 - a_2)\pi\nu^2}{2(a_3 - a_{10})n_2^2 \sinh\left(\dfrac{\pi\nu}{2n_2}\right)} \sin\nu t_0$$
$$- 2\hat{\gamma} G^{*2}[n_2 + a_2 \arctan(Z)].$$

Now, we can compute the second term M_2 of the complete Melnikov function. By substitution of Eqs. (18) and (21) into (23), this term M_2 may be written as

$$M_2 = -\hat{\gamma} \int_{-\infty}^{\infty} (a_2 \cos^2 l^* - a_{10} \sin^2 l^*)[a_3 L^{*2}$$
$$+ a_2(G^{*2} - L^{*2}) + (a_{10} - a_2)$$
$$\times (G^{*2} - L^{*2}) \sin^2 l^*]dt + \hat{\gamma} a_2 \int_{-\infty}^{\infty} [a_3 L^{*2}$$
$$+ a_2(G^{*2} - L^{*2}) + (a_{10} - a_2)$$
$$\times (G^{*2} - L^{*2}) \sin^2 l^*]dt.$$

In order to avoid terms that would produce unbounded results for M_2, the last two integrals must be grouped in only one integral. In this way, M_2 is given by

$$M_2 = \hat{\gamma}(a_2 - a_{10}) \int_{-\infty}^{\infty} [a_3 L^{*2} \sin^2 l^*$$
$$+ a_2(G^{*2} - L^{*2}) \sin^2 l^*$$
$$+ (a_{10} - a_2)(G^{*2} - L^{*2}) \sin^4 l^*]dt.$$

Making use of Eqs. (12) to express M_2 in the (G_x, G_y, G_z) variables, we obtain

$$M_2 = \hat{\gamma}(a_2 - a_{10}) \int_{-\infty}^{\infty} \left[a_3 \frac{G_x^{*2} G_z^{*2}}{G_x^{*2} + G_y^{*2}} + a_2 G_x^{*2} + (a_{10} - a_2) \frac{G_x^{*4}}{G_x^{*2} + G_y^{*2}} \right] dt$$
$$= \hat{\gamma}(a_2 - a_{10})[a_3 I_2 + a_2 I_4 + (a_{10} - a_2)I_5]. \tag{29}$$

We have already computed integral I_2 in Eqs. (27) and (28). Taking into account Eqs. (4), the other two integrals I_4 and I_5 become

$$I_4 = \int_{-\infty}^{\infty} G_x^{*2} dt = G^{*2}\left(\frac{a_3 - a_2}{a_3 - a_{10}}\right) \int_{-\infty}^{\infty} \operatorname{sech}^2(n_2 t)dt = G^{*2}\frac{2(a_3 - a_2)}{n_2(a_3 - a_{10})},$$

$$I_5 = \int_{-\infty}^{\infty} \frac{G_x^{*4}}{G_x^{*2} + G_y^{*2}} dt = G^{*2}\left(\frac{a_3 - a_2}{a_3 - a_{10}}\right)^2 \int_{-\infty}^{\infty} \frac{dt}{\cosh^2(n_2 t)[D + \sinh^2(n_2 t)]},$$

$$I_5 = G^{*2}\frac{2(a_3 - a_2)^3}{n_2^3(a_{10} - a_3)}\left[1 - \frac{a_3 - a_{10}}{n_2} \arctan(Z)\right].$$

Therefore, substituting the results of I_2, I_4 and I_5 into Eq. (29), the function M_2 yields

$$M_2 = 2\hat{\gamma} G^{*2} a_2 \arctan(Z).$$

Thus, the complete Melnikov function $M(t_0)$ of the system under both perturbations, finally results in

$$M(t_0) = M_1 + M_2 = G^{*2}\left[\frac{G^*(a_3 - a_2)\pi\nu^2}{2(a_3 - a_{10})n_2^2 \sinh\left(\dfrac{\pi\nu}{2n_2}\right)} \sin\nu t_0 - 2\hat{\gamma} n_2 \right]. \tag{30}$$

It is important to note that Eq. (30) give us an analytical criterion for heteroclinic chaos in terms of the system parameters. Indeed, from (30) it is easy to derive that the Melnikov function $M(t_0)$ has simple zeroes for

$$\hat{\gamma} < \hat{\gamma}_c = \frac{G^*(a_3 - a_2)\pi\nu^2}{4(a_3 - a_{10})n_2^3 \sinh\left(\dfrac{\pi\nu}{2n_2}\right)}, \qquad (31)$$

that is, for $\hat{\gamma} < \hat{\gamma}_c$ the perturbations produce chaotic behavior near the unperturbed separatrix. On the other hand, for $\hat{\gamma} > \hat{\gamma}_c$, the Melnikov function $M(t_0)$ is bounded away from zero, and hence there are no heteroclinic intersections and no chaos in the perturbed system.

Taking into account that $\hat{\gamma} = \gamma/\varepsilon$, analytical criterion (31) for chaotic behavior can be expressed in terms of γ, ε and ν as

$$\gamma < \gamma_c = \frac{\varepsilon G^*(a_3 - a_2)\pi\nu^2}{4(a_3 - a_{10})n_2^3 \sinh\left(\dfrac{\pi\nu}{2n_2}\right)}. \qquad (32)$$

It is worth to note that γ_c is directly proportional to the width of the stochastic layer in the absence of external viscous drag. Indeed, the width of the layer is proportional to the Melnikov integral M_{11} (25), so that γ_c can be written as

$$\gamma_c = \frac{1}{n_2 G^{*2}} M_{11}.$$

This fact proves that the wider the layer the bigger the value of γ_c and then, to eliminate the chaotic

behavior a stronger drag is necessary for a wider stochastic layer. Also note that the variation of γ_c as a function of the parameters ε and ν will be the same as M_{11}. In this way, keeping ε constant and varying the frequency ν we observe that γ_c goes to 0 as $\nu \longrightarrow 0$ or $\longrightarrow \infty$, that is to say, in the two integrable limits of the problem. This is a consistent result with the predicted behavior of the system.

5. Numerical Simulations

In the previous section, we have obtained, by means of the Melnikov's method, an analytical criterion (32) for the existence of heteroclinic chaos in terms of the system parameters γ, ε, ν and a_i. In order to check the validity of this analytical criterion we have studied the time-evolution of the perturbed system through computer numerical simulations by numerical integration of the equations of motion (15) by means of a Runge–Kutta algorithm of fifth order with fixed step [Lambert, 1976, pp. 121–123]. In this way, we look for a numerical criterion for chaotic or regular behavior.

We observe, by plotting a trajectory in the (l, L) planar reduced phase space of the perturbed system, two different classes of trajectories basically. On the one hand, trajectories that simply decay to one of the two stable fixed points $(l, L) = (\pm\pi/2, 0)$ without crossing themselves (Fig. 8 shows a representative example of this kind of regular trajectories for $\gamma = 0.01$, $\varepsilon = 0.01$ and $\nu = 0.1$ with
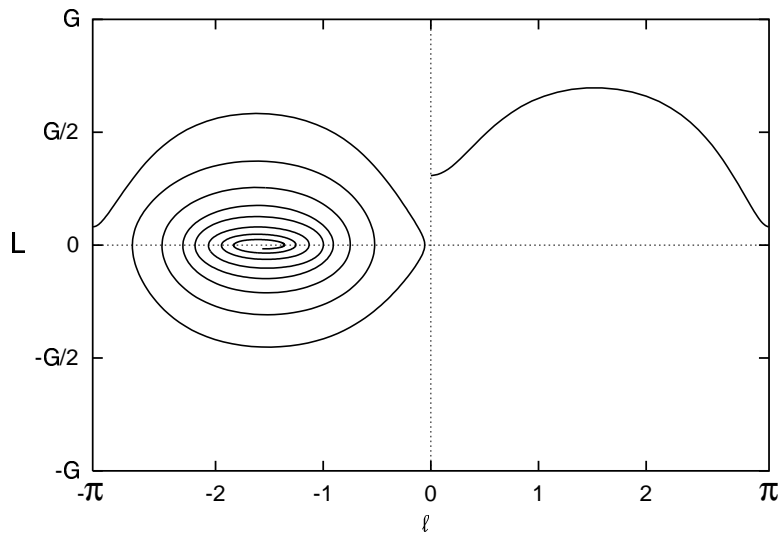

Fig. 8. Representative example of a regular trajectory where $\gamma = 0.01$, $\varepsilon = 0.01$, $\nu = 0.1$, $a_{10} = 0.1$, $a_2 = 0.2$, $a_3 = 0.3$ and with initial conditions $l_0 = 0$, $L_0 = 0.31$, $G_0 = 1$.
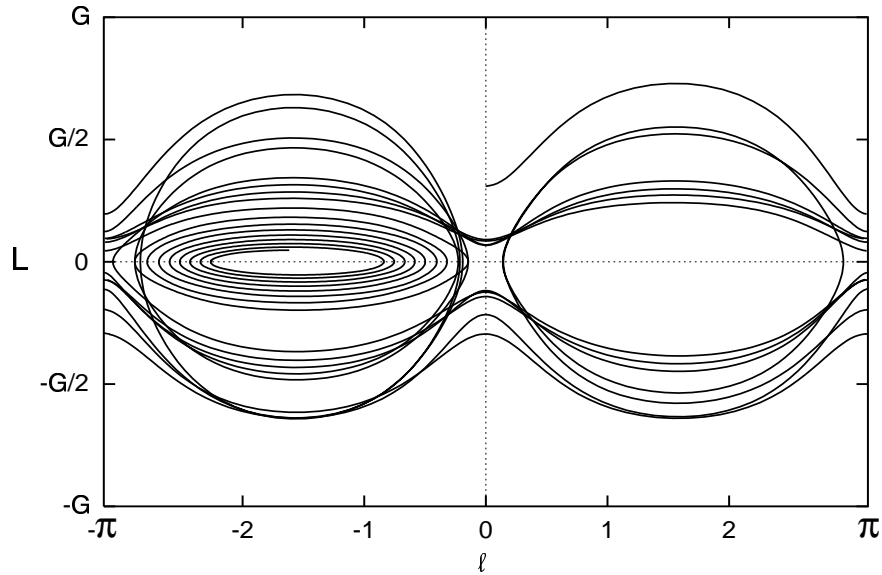
Fig. 9.   Representative example of a chaotic trajectory where $\gamma = 0.002$, $\varepsilon = 0.01$, $\nu = 0.1$, $a_{10} = 0.1$, $a_2 = 0.2$, $a_3 = 0.3$ and with the same initial conditions as Fig. 8.

initial conditions $l_0 = 0$, $L_0 = 0.31$, $G_0 = 1$). On the other hand, trajectories that cross themselves in the initial period of the decay before approaching an attracting fixed equilibrium as it can be seen in Fig. 9, for $\gamma = 0.002$ and the same parameters values and initial conditions as in Fig. 8. It is the last kind of trajectories that seem to exhibit a transient chaotic behavior in their initial evolution near the separatrix of the unperturbed problem. In this way, we consider a selfcrossing trajectory as a chaotic one while a nonselfcrossing trajectory is considered as a regular one.

It is worth to note that regular orbits are found whatever the values of the parameters, while the appearance of chaotic orbits is strongly related with the value of the parameters. Therefore, if for given values of γ, ε and ν we find a selfcrossing trajectory, it can be said that the system has a local transient chaotic behavior for those parameter values. Otherwise, we can say that the system has a regular behavior. Taking this into account, we are in a position to establish a numerical criterion for chaotic behavior. This allows us to determine a critical value γ_c such that for $\gamma > \gamma_c$ all the orbits are regular, while for $\gamma < \gamma_c$ there are chaotic orbits.

At this point, we are able to compare both the numerical and analytical values of γ_c that determine the transition between chaotic and regular regimes. In order to do this, we have designed a suitable algorithm to detect self-intersecting trajectories, that

is to say chaotic ones. For each set of values of the system parameters, we have swept the axis $l = 0$ from $L = G = 1$ to $L = 0$ with steps of 10^{-2} looking for initial conditions of chaotic trajectories. It is known that for $\gamma = 0$ the system exhibits chaotic behavior. So, as we are interested in finding γ_c as a function of ε and ν, we increased γ from zero with steps of $5 \cdot 10^{-4}$, for constant values of ε and ν. The first value of γ for which we find no chaotic trajectory give us a numerical estimation of γ_c.

Figures 10 and 11 show the comparison between the analytical and the numerical estimations of the critical value γ_c for an asymmetric body with $a_{10} = 0.1$, $a_2 = 0.2$ and $a_3 = 0.3$. Figure 10 shows
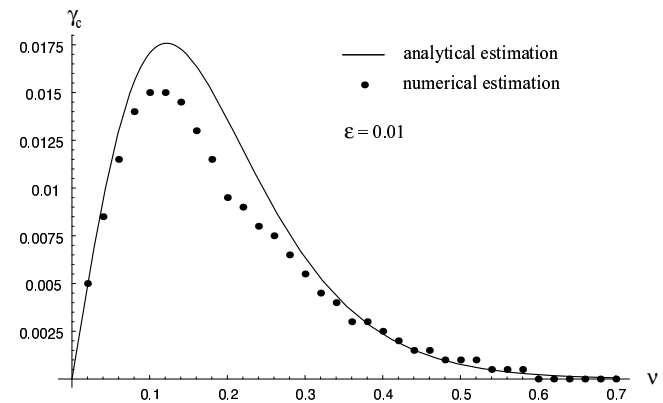

Fig. 10.   Comparative evolution of the estimations of γ_c as a function of the frequency ν for a fixed amplitude $\varepsilon = 0.01$, and for $a_{10} = 0.1$, $a_2 = 0.2$, $a_3 = 0.3$.
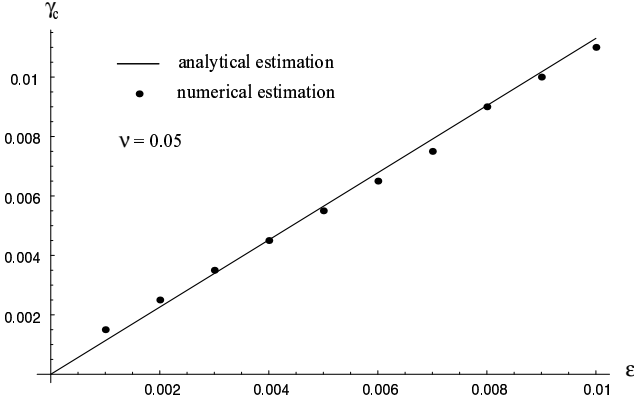
Fig. 11. Comparative evolution of the estimations of γ_c as a function of the amplitude ε for a fixed frequency $\nu = 0.05$, and for $a_{10} = 0.1$, $a_2 = 0.2$, $a_3 = 0.3$.

both estimations of γ_c as functions of ν, for a fixed amplitude value $\varepsilon = 0.01$. On the other hand, Fig. 11 presents the estimations of γ_c as a function of the amplitude ε for constant frequency $\nu = 0.05$.

Figure 10 shows that, for fixed amplitude ε, there is a great agreement between the analytical estimation of γ_c, predicted in Eq. (32), and the numerical estimation. This agreement is specially good for high and low values of frequency ν. Nevertheless,

for intermediate values of ν we observe a slight disagreement between the two estimations in such a way that the analytical estimation predicts chaotic behavior for γ varying in a bigger range. This fact can be owing to the criterion to determine γ_c numerically by means of the occurrence of self-crossing orbits in the (l, L) plane or to a missing chaotic orbit while sweeping the L axis.

It is worth to note that Fig. 10 also reveals the two integrable limits of the perturbed problem: for $\nu = 0$ and for $\nu \to \infty$. It may be observed that as $\nu \longrightarrow \infty$ and $\nu \longrightarrow 0$ γ_c tends to zero, that is, the chaotic behavior tends to disappear in the integrable limits.

Also great agreement is obtained for fixed values of frequency ν while varying the amplitude ε, as can be seen in Fig. 11 for a low fixed value of the frequency $\nu = 0.05$. Thus, the predicted behavior of Eq. (32) is confirmed by the numerical estimation: for a fixed frequency ν the critical viscous drag coefficient γ_c grows linearly with the amplitude ε of the perturbation.

Both numerical and analytical criterion show, with very good agreement, the existence of chaotic behavior for given values of the parameters ε and ν despite $\gamma < \gamma_c$. This chaotic behavior is not
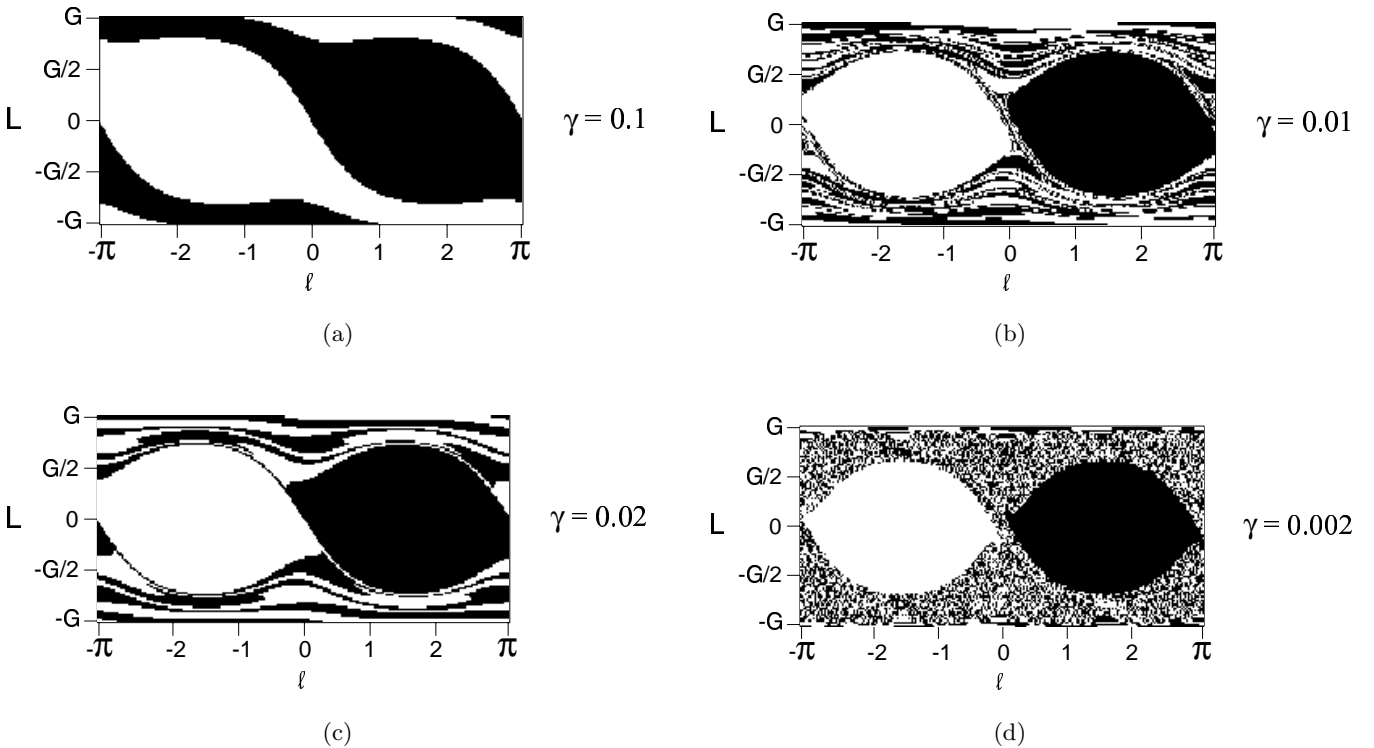

(a)

(b)

(c)

(d)

Fig. 12. The geometric structure of the attraction basins as a function of γ.

only reflected in the presence of self-crossing orbits but, as we will see, in a very random asymptotic behavior. As it is known, the main contribution of the viscous drag is to despin the body. So, it does not matter what the initial conditions are, the final state of the body is at rest with the spinning axis pointing well to the positive direction of the b_1 axis or to the negative direction of the b_1 axis. That is to say, the two fixed points located at the b_1 axis are two sinks for the system.

We focus on the geometry of the attraction basin of the two sinks depending on the parameters of the system. In this way, for given values of ε and ν, we tune γ from the regular regime ($\gamma > \gamma_c$) to the chaotic one ($\gamma < \gamma_c$) with the aim to detect changes in the geometrical structure of the basins. Figure 12 shows how the basins look like as γ varies from the regular regime to the chaotic one. We note that for regular behavior the two attraction basins are well defined and separated by smooth curves in phase plane. Thus, given an initial condition, it is possible to decide the w-limit point of the orbit through it, that is, the final state of the system. On the contrary, for chaotic behavior the attraction basins are no longer well defined and we find areas where the two basins merge. These mixing areas are bigger as the chaotic behavior increases, that is, for small values of γ.

Note that the basins are mainly destroyed outside the separatrix while inside it two well defined basins remain. This fact is owing to the different nature of the orbits inside and outside of the separatrix. Inside orbits are not affected by homoclinic chaos except those orbits that initially lie on the stochastic layer. On the other hand, outside orbits necessarily have to cross the separatrix to reach one of the two attractors. So, the longer the time an orbit spends in chaotic regime (surrounding the separatrix inside the stochastic layer) the more the uncertainty to know the final state. Thus, for small values of γ the points of the attraction basin of each of the two sinks are distributed at random outside the separatrix as well along the primary stochastic layer, as can be seen in Fig. 12 for $\gamma = 0.002$.

6. Conclusions

We have established an analytical criterion for the existence of transient heteroclinic chaos in terms of the system parameters for a rotating asymmetric body with a time-dependent moment of inertia and under the action of a small external viscous drag. The analytical criterion for the transient chaotic behavior has been obtained applying a higher dimensional generalization of the Melnikov's method to a perturbed asymmetric rigid body model with three degrees of freedom. In addition, we have studied numerically the dynamics of the perturbed system by means of computer simulations. This numerical research was confirmed with substantial agreement from the analytical results given by the Melnikov's method.

References

Bryson, A. E. [1988] *Control of Spacecraft and Aircraft* (Princeton University Press, Princeton).

Deimel, R. F. [1952] *Mechanics of the Gyroscope. The Dynamics of Rotation* (Dover, NY).

Deprit, A. & Elipe, A. [1993] "Complete reduction of the Euler–Poinsot problem," *J. Astron. Sci.* **41**, 603–628.

Gradshteyn, I. S. & Ryzhik, I. M. [1980] *Table of Integrals, Series and Products* (Academic Press, San Diego).

Gray, A. [1959] *A Treatise on Gyrostatics and Rotational Motion* (Dover, NY).

Gray, G. L., Kammer, D. C., Dobson, I. & Miller, A. J. [1999] "Heteroclinic bifurcations in rigid bodies containing internally moving parts and a viscous damper," *J. Appl. Mech. — Trans. ASME* **66**, 720–728.

Guckenheimer, J. & Holmes, P. [1983] *Nonlinear Oscillations, Dynamical Systems and Bifurcations of Vector Fields* (Springer-Verlag, NY).

Holmes, P. J. & Marsden, J. E. [1983] "Horseshoes and Arnold diffusion for Hamiltonian systems on Lie groups," *Indiana Univ. Math. J.* **32**, 273–309.

Hughes, P. C. [1986] *Spacecraft Attitude Dynamics* (John Wiley, NY).

Iñarrea, M. & Lanchares, V. [2000] "Chaos in the reorientation process of a dual-spin spacecraft with time-dependent moments of inertia," *Int. J. Bifurcation and Chaos* **10**, 997–1018.

Koiller, J. [1984] "A mechanical system with a "wild" horseshoe," *J. Math. Phys.* **25**, 1599–1604.

Lambert, J. D. [1976] *Computational Methods in Ordinary Differential Equations* (John Wiley, London).

Lanchares, V., Iñarrea, M. & Salas, J. P. [1998] "Spin rotor stabilization of a dual-spin spacecraft with time dependent moments of inertia," *Int. J. Bifurcation and Chaos* **8**, 609–617.

Leimanis, E. [1965] *The General Problem of the Motion of Coupled Rigid Bodies About a Fixed Point* (Springer-Verlag, Berlin).

Lichtenberg, A. J. & Lieberman, M. A. [1992] *Regular and Chaotic Dynamics*, 2nd edition (Springer-Verlag, NY).

Melnikov, V. K. [1963] "On the stability of the center for time periodic perturbations," *Trans. Moscow Math. Soc.* **12**, 1–56.

Peano, G. [1895a] "Sopra lo spostamento del polo sulla terra," *Atti. R. Accad. Sci. Torino* **30**, 515–523.

Peano, G. [1895b] "Sul moto del polo terrestre," *Atti. R. Accad. Sci. Torino* **30**, 845–852.

Peng, J. & Liu, Y. [2000] "Chaotic motion of a gyrostat with asymmetric rotor," *Int. J. Nonlin. Mech.* **35**, 431–437.

Salam, F. M. A. [1987] "The Melnikov technique for highly dissipative systems," *SIAM J. Appl. Math.* **47**, 232–243.

Serret, J. A. [1866] "Mémoire sur l'emploi de la méthode de la variation des arbitraires dans la théorie des mouvements de rotation," *Mémoires de l'académie des sciences de Paris* **35**, 585–616.

Sidi, M. J. [1997] *Spacecraft Dynamics and Control* (Cambridge University Press, NY).

Tong, X., Tabarrok, B. & Rimrott, F. P. J. [1995] "Chaotic motion of an asymmetric gyrostat in the gravitation field," *Int. J. Nonlin. Mech.* **30**, 191–203.

Volterra, V. [1899] "Sur la théorie des variations des latitudes," *Acta Math.* **22**, 201–358.

Wainwright, L. [1927] "On damping effects in exterior ballistics," *Philos. Mag.* **3**, 641–660.

Wiesel, W. E. [1997] *Spaceflight Dynamics*, 2nd edition (McGraw-Hill, NY).

Wiggins, S. [1988] *Global Bifurcations and Chaos: Analytical Methods* (Springer-Verlag, NY).

Wisdom, J., Peale, J. & Mignard, F. [1984] "Chaotic rotation of hyperion," *Icarus* **58**, 137–152.